Available online at www.sciencedirect.com
SCIENCE DIRECT
Polymer 46 (2005) 12567–12576
polymer
www.elsevier.com/locate/polymer

Moisture absorption in polyamide-6 silicate nanocomposites and its influence on the mechanical properties

D.P.N. Vlasveld [a,b], J. Groenewold [a,b], H.E.N. Bersee [c], S.J. Picken [a,b,*]

[a] Polymer Materials and Engineering, Faculty of Applied Sciences, Delft University of Technology, Julianalaan 136, 2628 BL Delft, The Netherlands
[b] Dutch Polymer Institute, John F. Kennedylaan 2, P.O. Box 902, 5600 AX Eindhoven, The Netherlands
[c] Design and Production of Composite Structures, Faculty of Aerospace Engineering, Delft University of Technology, Kluyverweg 3, P.O. Box 5058, 2600 GB Delft, The Netherlands

Received 1 April 2005; received in revised form 22 July 2005; accepted 20 October 2005
Available online 10 November 2005

Abstract

The influence of the amount of silicate and the amount of absorbed moisture on the mechanical properties of PA6 nanocomposites is discussed. Diffusion coefficients have been determined from moisture absorption experiments and similar amounts of water were absorbed by nanocomposites with different silicate concentrations. The modulus of the nanocomposites increases with increasing amount of silicate and decreases with increasing amount of absorbed moisture. However, the ductility of the nanocomposites decreases with increasing amount of silicate and increases with increasing moisture content. A more hydrophobic modification of the particles results in a reduction of the degree of exfoliation in PA6, and consequently in a lower modulus, higher ductility and an increased diffusion coefficient compared to particles that are better exfoliated. PA6 nanocomposites can compensate for the decrease of the modulus of PA6 when water is absorbed from the environment.

Keywords: Polyamide; Nanocomposite; Moisture absorption

1. Introduction

Polyamide 6 (PA6) is one of the most used types of aliphatic polyamide. The main applications of PA6 are in fibres, films, and as injection-moulded engineering plastic. PA6 crystallizes fast, usually up to percentages in the range of 30–40%, providing a high modulus to the material even above the glass transition temperature (T_g). One property common to all polyamides is that they absorb water from the environment, both from the air and from liquid water. The equilibrium moisture content of PA6 at 23 °C in a 50% relative humidity environment is around 2.5 wt% and at 100% relative humidity as high as 9 wt% [1]. Absorbed water in polyamide has a large influence on many properties: decrease of T_g, modulus and yield stress, while both elongation at break and toughness increase [1]. PA6 is often filled with mineral fillers or short fibres such as glass, carbon or aramid fibres to increase the modulus. With the addition of rigid fillers the decrease of the modulus under the influence of water can be compensated. The addition of this type of fillers can be very effective when the polymer is used as an engineering plastic in injection-moulded products. Filler levels up to 60 vol% are possible, leading to very stiff materials. However, for fibre and film applications these types of fillers are not very useful, because the relatively large size of the filler particles has a negative influence on the toughness, transparency and surface appearance. In addition, high contents of traditional mineral and glass fillers lead to a large increase in the density of the compound.

To overcome the disadvantages of traditional reinforcements, approximately a decade ago layered silicate nanocomposites were developed. The extremely small filler particles in nanocomposites provide several advantages compared to traditional filled compounds, such as lower amounts of fillers and, therefore, lower density, increased barrier properties, improved transparency and better surface appearance.

Nanocomposites consisting of exfoliated silicate layers in PA6 can be produced by in situ polymerization, in which organically modified silicate layers were swollen by

* Corresponding author. Address: Polymer Materials and Engineering, Faculty of Applied Sciences, Delft University of Technology, Julianalaan 136, 2628 BL Delft, The Netherlands. Tel.: +31 15 278 6946; fax: +31 15 278 7415.
E-mail address: s.j.picken@tnw.tudelft.nl (S.J. Picken).

0032-3861/$ - see front matter © 2005 Elsevier Ltd. All rights reserved.
doi:10.1016/j.polymer.2005.10.096

the monomer for PA6 (ε-caprolactam) and exfoliated during polymerization [2–4], or by dispersion in the melt by high shear mixing in a twin-screw extruder [5–8].

Because of the large aspect ratio and surface area of the exfoliated silicate layers they act as efficient barriers against transport through the material [9]. The transport speed of gasses and vapours through the polymer is reduced because the impenetrable silicate layers cause an increase in the path length for molecules diffusing through the polymer [10,11]. The reduced transport rate reduces the rate of moisture uptake in hydrophilic polymers such as PA6. Because absorption of water reduces the glass transition temperature and the modulus of PA6, the addition of nanoparticles to reduce the negative effects of water uptake is particularly useful. The nanoparticles influence the properties of moisture-conditioned nanocomposites in two ways: they reduce the water uptake speed due to the barrier properties, and they increase the modulus of the plasticized nanocomposite.

Despite the importance of the influence of moisture in practical applications, only a few papers containing data for mechanical properties of moisture-conditioned nanocomposites have been published [7,11–15]. However, for a complete understanding of polyamide nanocomposites it is important to understand both how the moisture absorption takes places and how this influences the mechanical properties. In this paper the influence of the type and amount of layered silicate and the relative humidity on the diffusion coefficient and the maximum amount of absorbed moisture is described. In addition, the influence of different amounts of moisture on the mechanical properties are measured and discussed. From the ratio of diffusion coefficients in the matrix and the nanocomposites the aspect ratio of the particles is calculated. The aspect ratio of the exfoliated particles is a very important factor that determines both the moisture transport rate and the elastic modulus of the nanocomposite.

2. Experimental

2.1. Materials

The polymer used to produce melt-blended nanocomposites is an injection-moulding grade of PA6, Akulon® K122D from DSM, The Netherlands.

Three organically modified platelet-shaped silicates were used, the first two based on purified natural montmorillonite clay, and the third on a synthetic layered silicate:

- Cloisite® 30 B from Southern Clay Products, USA (Montmorillonite). Surfactant: methyl bis-2-hydroxyethyl tallow quaternary ammonium(32 wt%).
- Nanomer® I 30 TC from Nanocor, USA (Montmorillonite). Surfactant: tri-methyl tallow quaternary ammonium (33 wt%).
- Somasif® MAE from Co-op Chemicals, Japan (Synthetic Mica®). Surfactant: di-methyl di-tallow quaternary ammonium (40 wt%).

The manufacturers have added organic surfactants on the silicate platelets to enhance the exfoliation, because they increase the layer distance and improve the interaction with the polymer. The amount of organic surfactant was determined with thermo-gravimetric analysis (TGA) in a Perkin–Elmer TGA-7 thermal gravimetric analyzer at 800 °C for 1 h in air.

2.2. Preparation

2.2.1. Extrusion

The nanocomposites were prepared by mixing organically modified silicate nanofillers in PA6 in a Werner and Pfleiderer ZDS-K28 co-rotating twin-screw extruder. The modified silicate powder was mixed with the PA6 granules and fed into the extruder at a constant rate via a Plasticolor 2500 feeding unit. The extruder was operated at a screw speed of 200 rpm and a feeding rate of approximately 3 kg/h, which resulted in an average residence time of 3 min in the extruder.

Temperature in the feeding zone was 150 °C, all the other zones where heated to 230 °C. Cooling was applied to keep the temperature constant, because the high shear in the melt can produce too much heat. First a master batch was made with a silicate content of approximately 10 wt% (based on the inorganic content of the silicate), and the other concentrations were made by mixing this master batch with unfilled K122D in a second extrusion step.

2.2.2. Injection moulding

Dumbbell shaped samples according to ISO 527 standards were injection moulded on an Arburg Allrounder 221-55-250 injection-moulding machine. The feeding zone was heated to 150 °C, the melting and mixing zones were heated to 240 °C and the nozzle was kept at 260 °C. The mould was heated to a temperature of 90 °C to reduce the cooling speed and ensure a more homogeneous crystallisation.

2.2.3. Determination of silicate content

Thermogravimetric analysis (TGA) measurements were used to determine the exact silicate content in the tested samples after processing. A Perkin–Elmer TGA-7 thermal gravimetric analyser was used to determine the weight fraction of silicate by heating a sample in air at 800 °C for 1 h.

2.2.4. Moisture conditioning

Dry as moulded samples were dried in a vacuum oven at 80 °C for at least 48 h before testing.

The moisture conditioning was performed at 70 °C to increase the speed of moisture transport. The sample weight was measured after drying and conditioning on a Mettler AE-240 to calculate the moisture level. The moisture content was calculated based on the amount of matrix material (PA6 and surfactant), so the weight of the silicate phase was not included.

Samples containing 3% water were prepared by conditioning in a Heraeus climate chamber at 70 °C and 65% relative humidity and samples containing 6% water were prepared by conditioning at 70 °C and 92% relative humidity.

The samples that were tested for the maximum moisture content and the mechanical properties were stored in these conditions until a constant weight was obtained, which indicated that the equilibrium moisture content was reached. This took different times for different silicate contents, and could take up to 10 weeks for the highest silicate content.

Several samples were stored without further treatment for 270 days in a room with an average temperature of 20 °C and an average relative humidity of 50%, which resulted in a variable moisture content depending on the silicate content. The diffusion coefficients were determined from rectangular samples of 27×20×4 mm, cut from the wide part of the ISO 527 test bars.

2.3. Testing

2.3.1. Mechanical properties

The samples were tested on a Zwick 1445 tensile tester with a 10 kN force cell. For the modulus measurement Zwick clip-on extensometers were used. The test speed was 5 mm/min and the temperature was 23 °C.

2.3.2. Crystallinity and volume fractions

The level of crystallinity of the samples was determined with differential scanning calorimetry on a Perkin–Elmer DSC-7. DSC samples of approximately 5 mg were cut from the centre of the tensile test bar. The DSC measurements were performed at a heating rate of 10 °C/min between 25 and 270 °C. The crystallinity was calculated using a heat of fusion of 213 J/g for the gamma crystals, and 243 J/g for the alpha crystals [16]. The volume fractions are calculated from the mass fractions by using the following densities: ρ surfactant = 0.93 g/cm^3 [17], ρ amorphous PA6 = 1.08 g/cm^3, ρ α-crystalline PA6 = 1.24 g/cm^3, ρ γ-crystalline PA6 = 1.18 g/cm^3 [1,18], ρ silicate = 2.8 g/cm^3 (equal to the density of mica [19]) (more details in Ref. [15]).

3. Theory

3.1. Water diffusion in polymers and nanocomposites

The moisture absorption speed in polymers and nanocomposites can be quantified by determining the diffusion coefficient. Fick's second law of diffusion (Eq. (1)) describes the accumulation of water in a sample as a function of time with a diffusion coefficient D [20].

$$\frac{\partial c}{\partial t} = \frac{\partial}{\partial x}\left(D\frac{\partial c}{\partial x}\right) \tag{1}$$

In the initial stage of the absorption, up to approximately $M_t/M_\infty \cong 0.5$, the increase in mass shows a linear relationship with the square root of time [20]. M_t is the mass increase of the sample at time t, and M_∞ the final mass increase of the sample at saturation. In this initial absorption phase, the diffusion profiles on the different sides of the sample do not overlap and develop independently. Therefore, as long as the diffusion profiles do not overlap, the mass flux of moisture, j, and its time dependence through the sample surface is the same everywhere and is equal to the flux of a semi infinite geometry:

$$j = \Delta c\sqrt{\frac{D}{\pi t}} \tag{2}$$

Here Δc is the difference in mass density of the initial (free of moisture) and the final (saturated) stage. To get the change in sample mass per unit time one has to integrate the flux over the surface of the sample. If the diffusion profiles that arise by penetration of moisture from the different sides of the sample do not overlap the flux through the sample surface is the same everywhere. As stated previously, significant overlap does not occur up to $M_t/M_\infty \cong 0.5$ [20]. Up to that point, the time derivative of the sample mass is given simply by the flux times the total surface area, A_{tot}. The value of the flux is then given by that of a semi-infinite geometry in Eq. (2). By integration of the flux times the area one finds for the mass increase:

$$\frac{M_t}{M_\infty} \cong \frac{2A_{tot}}{V}\sqrt{\frac{Dt}{\pi}} \tag{3}$$

where A_{tot} is the total area of the sample and V the total volume. In Eq. (3) the fact has been used that the final mass of the sample is given by $M_\infty = \Delta cV$. Eq. (3) can be used to calculate the diffusion coefficient of a polymer or nanocomposite by plotting (M_t/M_∞) versus $\sqrt{t}$. Then by using Eq. (3) the diffusion coefficient can be determined from the slope. Since we analyze dogbone samples and not films we use the generalized equation for the mass increase where the total area and volume of the sample are significant parameters. The region of validity where the mass increase scales with the square root of time now is slightly less than that of a slab geometry. In our analysis we will restrict to the data points that follow the square root law to determine the diffusion coefficient. The speed of water absorption in PA6 nanocomposites is reduced compared to the unfilled polymer because of the impermeable silicate layers in the polymer. These layers increase the path-length for diffusion through the polymer [21]. This increased path length predicts the better barrier properties of nanocomposites very well [16]. Contrary to what is sometimes suggested [13], the amount of water that can be absorbed by PA6 nanocomposites is not reduced; only the rate of absorption is reduced due to the lower diffusion coefficient [11]. In PA6 the water is absorbed in the amorphous phase, because the crystalline part is inaccessible for water [1]. The amorphous fraction is not much different in nanocomposites [10,15,22] and, therefore, the amount of absorbed water can reach approximately the same level as in unfilled polyamide, if sufficient time is available. However, data obtained according to (for example) the ISO-62 or ASTM D570-98 standards can give the impression that nanocomposites absorb less moisture. These standards describe procedures in which the moisture absorption is performed in a fixed time, with a maximum of 24 h, which is clearly not adequate to compare nanocomposites and unfilled polymers. Due to the lower transport rate nanocomposites do not reach the equilibrium moisture content within the fixed time (depending

on the sample thickness and conditioning temperature), which was probably the reason for the low moisture absorption reported in several articles [13,14]. Only repeated measurement of the weight increase during moisture absorption until no more increase is observed can ensure that the equilibrium moisture content has been reached.

The diffusion coefficients D can be used to compare the diffusion speed in the unfilled polymer and nanocomposite and to estimate how much time total moisture saturation of a sample takes, depending on the dimensions. In addition, it is possible to calculate the aspect ratio of the silicate sheets in the nanocomposites from the ratio of diffusion coefficients of the nanocomposite and the matrix. Nielsen [21] has derived a simple theory, which relates the diffusion coefficient to the increased path that molecules have to travel when diffusing around impenetrable platelets. Many simplifications have been made in this theory, which reduce the accuracy of the results. An important difference between Nielsen's model and real nanocomposites is the fact that Nielsen's theory is a two-dimensional theory in which the third dimension of the plates is considered infinitely long. In addition, it assumes perfectly overlapping ribbons, while real particles are randomly oriented, at least in the long dimensions of the platelets. Therefore, this theory underestimates the real diffusion coefficient. Van Es [16] has derived a more accurate equation for diffusion in nanocomposites filled with aligned platelets, which is based on a combination of models by Brydges et al. [23] and Hatta et al. [24]:

$$\left(\frac{D_{\text{matrix polymer}}}{D_{\text{nanocomposite}}}\right) = (\varphi_{\text{filler}}\beta + 1 - \varphi_{\text{filler}})(\varphi_{\text{filler}}\beta\gamma(1-\gamma) + 1) \tag{4}$$

$$\beta = \frac{8}{5\pi}\frac{w}{t} \qquad \frac{w}{t} = \text{width/thickness} = \text{aspect ratio platelets}$$

γ = overlap factor; $\gamma = 0.5$ for perfect overlap of the platelets, 0 for no overlap and 0.25 for platelets that are randomly oriented in two-dimensions.

Eq. (4) is valid for diffusion with a wide variety of particle concentrations, and the validity was confirmed by comparison with three-dimensional finite element modelling. This equation is based on diffusion through a material around impenetrable platelets that are all aligned parallel to each other. This is a reasonable assumption in injection-moulded samples [25–27], especially on the outside of the sample where the first diffusion is measured. WAXS measurements on these nanocomposites have indeed shown highly oriented silicate layers [15]. However, within the plane of the platelets there is no specific ordering, so the random placement of the sheets leads to an overlap factor γ of 0.25 in this model.

3.2. Influence of water on mechanical properties

Absorbed moisture decreases T_g in PA6 and other polyamides [1] because the water molecules interfere with the hydrogen bonds between the polymer chains and this increases the chain mobility. The reduced T_g in the presence of water results in a strong reduction of the amorphous modulus in the temperature range around T_g, which leads to a decrease of the modulus of the semi-crystalline polymer. Because of the reduction of the matrix modulus, also polyamide nanocomposites suffer from a modulus reduction after moisture conditioning. In addition, the increased mobility reduces the yield stress and increases the ductility and elongation at break.

4. Results and discussion

Nanocomposites with a range of concentrations of layered silicate filler as shown in Table 1 were used. The silicate content shown in Table 1 are the quantities determined with TGA measurements.

4.1. Moisture absorption

The maximum moisture content absorbed by our samples was determined at 70 °C as a function of the relative humidity between 55 and 100% (Fig. 1). Two different moisture levels, 3 and 6 wt%, were chosen to measure the mechanical properties, which corresponds to moisture conditioning levels of 65 and 92% RH at 70 °C.

Water is only absorbed by the amorphous part of PA6 [1]. However, in nanocomposites containing organically modified layered silicate, the surfactant on the platelets can be considered as another amorphous fraction of the material, which can be mixed with the polymer. Therefore, the question arises if the moisture is absorbed by the PA6 phase only, or also by the surfactant. In Fig. 2(A) the moisture content in the different concentrations of Cloisite® 30 B nanocomposites after conditioning at 92% RH is shown, calculated with respect to the amorphous PA6 phase and with respect to the total amorphous matrix (amorphous PA6 and surfactant). The volume fractions of amorphous PA6, crystalline PA6, silicate and surfactant used in the calculation (calculated from TGA and DSC data) are shown in Fig. 2(B).

To be clear, we mean by '(total) sample' all four phases in Fig. 2(B), by '(total) matrix' everything except the silicate phase, by 'total amorphous matrix' amorphous PA6 + surfactant and by 'total PA6' amorphous PA6 + crystalline PA6.

Keeping in mind that the water concentration of approximately 9.5 wt% in the amorphous phase equals approximately 6 wt% water in the total matrix phase, Fig. 2(A) shows that nanocomposites can indeed absorb approximately the same equilibrium amount of moisture (in the total matrix) as unfilled

Table 1
Silicate content in the nanocomposites determined by TGA

Silicate type	Silicate content (wt%)				
Cloisite® 30B	2.6	4.7	6.8	8.3	10.6
Nanomer® I30T	2.5	4.4	6.6	8.3	10.2
Somasif® MAE	2.5	3.6	5.6	7.1	9.1

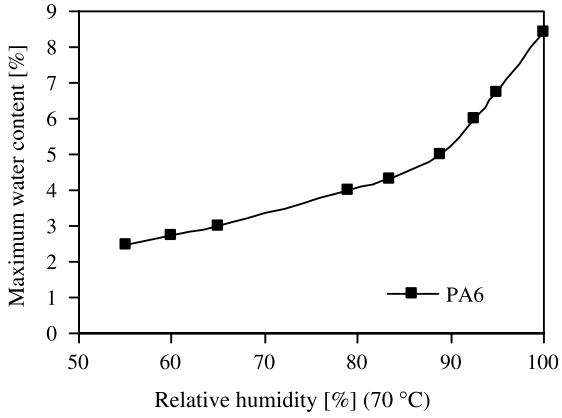

Fig. 1. Maximum water content in PA6 as a function of the relative humidity at 70 °C.

PA6. In addition, it shows that it is likely that the water is distributed in the total amorphous matrix, which includes the small fraction of surfactant in organically modified nanocomposites. If the water would only be in the amorphous PA6 phase, this would mean that an increase in silicate content would imply an increase in the moisture content, which is unlikely.

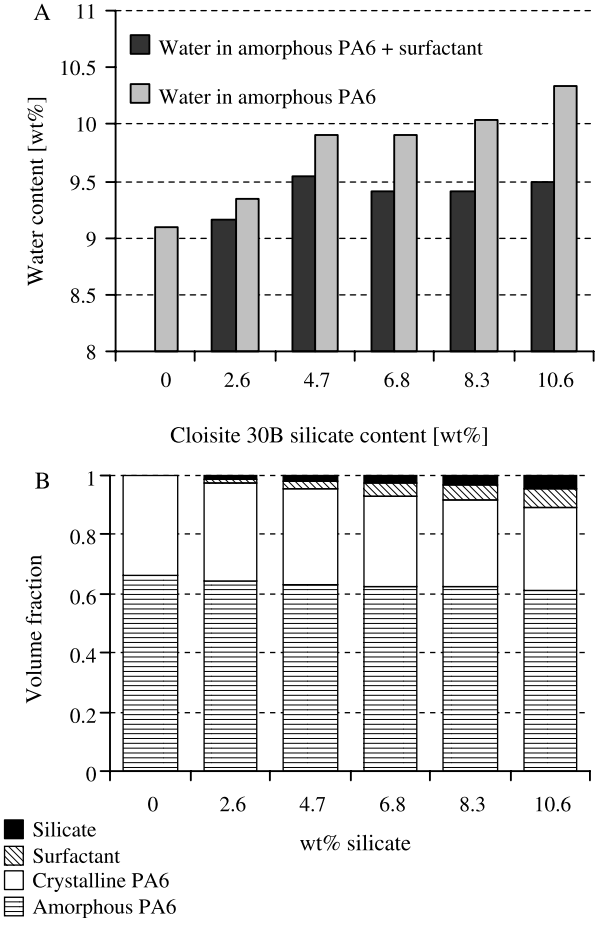

Fig. 2. (A) Equilibrium moisture content in the amorphous phase after 70 °C/92% RH conditioning, calculated with and without the surfactant phase. (B) Composition Cloisite® 30B nanocomposites (see for details Ref. [15]).

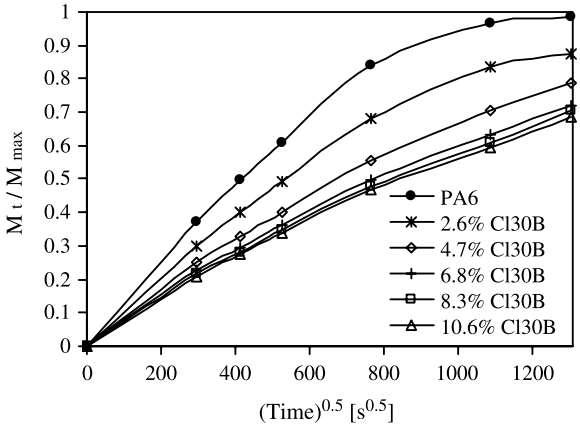

Fig. 3. Water absorption Cloisite® 30B nanocomposites at 70 °C/65% RH.

4.1.1. Diffusion coefficient

The increase in water content of the nanocomposites and unfilled PA6 was measured at 70 °C, both at 65 and 92% RH. An example is shown in Fig. 3 for Cloisite® 30B nanocomposites at 65% RH, where the absorption results are shown as $(\%_t/\%_{max})$ versus $\sqrt{t}$. It shows that the initially straight line levels off above $(\%_t/\%_{max}) > 50\%$.

The speed of moisture absorption is reduced with increasing amounts of exfoliated silicate, due to the barrier properties. Eq. (3) is used to calculate the diffusion coefficient form the slope in the initial part of the curve, which equals $((A_{total}/2V)(4/\sqrt{\pi}))\sqrt{D}$. The constant $(A_{total}/2V)(4/\sqrt{\pi})$ is equal to 771 for the samples used for the moisture absorption experiments.

From the slopes of the linear fit at low moisture content the diffusion coefficients are calculated for all nanocomposites at 65% RH and 92% RH. In Fig. 4 the diffusion coefficients are plotted versus silicate content. The Cloisite® 30B and Nanomer® I30TC nanocomposites show a similar strong decrease of the diffusion coefficient with increasing silicate content, while the Somasif® MAE nanocomposites show

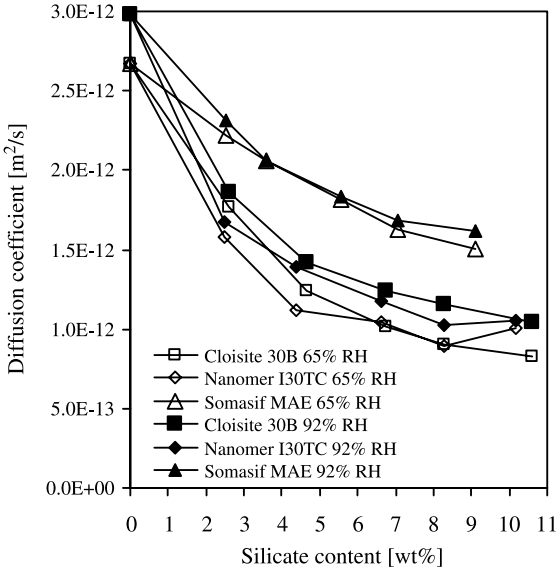

Fig. 4. Diffusion coefficients nanocomposites.

a smaller decrease. This is probably the result of reduced exfoliation and consequently smaller aspect ratios for the MAE nanocomposites. A lower compatibility of MAE particles due to the double surfactant chains leads to a less effective exfoliation and the presence of stacks of platelets, resulting in a lower effective particle aspect ratio. The diffusion coefficients at the highest silicate content are almost three times smaller than that of unfilled PA6, which means that the nanocomposites will take approximately three times longer to reach saturation. The results also show that the diffusion coefficient depends on the moisture content during conditioning. A higher relative humidity leads to a higher moisture content in the sample, and this leads to a higher diffusion coefficient. This concentration dependence is a known phenomenon in polyamides [1,28,29], which is caused by the swelling of the amorphous phase with the absorbed water. The effect is not very strong in our samples, probably because the absorption temperature (70 °C) is above the T_g of the material. In this case the absorption of water has less influence on the chain mobility, because the amorphous phase is already mobile at this temperature.

The influence of the temperature on the diffusion coefficient is much stronger than the influence of the moisture content. It has been shown that diffusion coefficient for water in PA6 has an exponential temperature dependence, with an activation energy $E_s = 0.49$ eV [28]:

$$D = D_0 \exp\left(-\frac{E_s}{kT}\right) \tag{5}$$

D_0 depends on variables such as the crystallinity. Eq. (5) is used to calculate the temperature dependence of D (Fig. 5), using the value we found at 70 °C and high RH ($D = 3.0 \times 10^{-12}$ m^2/s).

The diffusion coefficient is approximately 17 times smaller at 20 °C compared to 70 °C and the moisture saturation will take approximately 17 times longer at room temperature. Therefore, in normal atmospheric conditions (20 °C/50% RH) it will take a very long time to reach the equilibrium moisture concentration in the 4 mm thick samples. The unfilled PA6 samples reached total saturation at 70 °C in 3 weeks, so a rough estimation shows that it takes 1 year for total saturation at room temperature. Therefore, it is clear that accelerated absorption at elevated temperature is necessary to reach the desired water content in a reasonable time, especially in nanocomposites

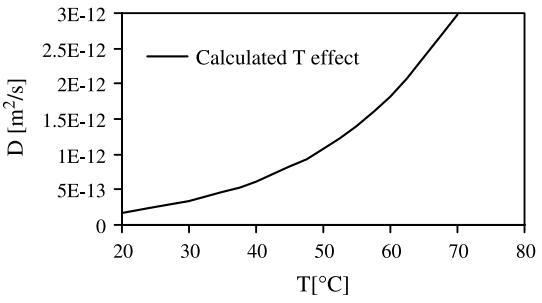

Fig. 5. Effect of the temperature on the diffusion coefficient in PA6, as calculated using Eq. (5).

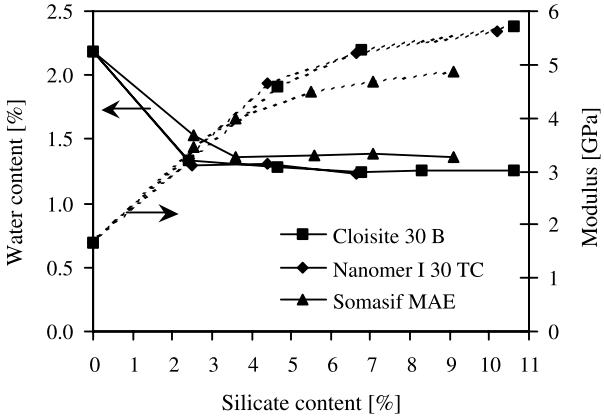

Fig. 6. Moisture content (solid lines) and modulus (dotted lines) after 270 days conditioning at approximately 20 °C and 50% RH.

where the diffusion coefficient is up to three times smaller than in unfilled PA6. This is illustrated by the moisture content of several samples that have been stored in a room with average conditions of 20 °C and 50% RH for 270 days. This resulted in moisture contents as shown in Fig. 6, (the concentrations are not the equilibrium moisture content; it is just one moment in a continuing process to reach equilibrium).

It can be seen that even the unfilled PA6 did not reach the equilibrium moisture content (ca. 2.5%) and the nanocomposites only reached half of this value in the available time. The strongest influence on the time required for total moisture saturation is the thickness of the samples, because Fick's second law results in a quadratic influence of the thickness on the time. When designing products with polyamide and its nanocomposites it is important to realize that the properties of the materials will continuously change in search of equilibrium over long time periods, up to several years.

These results make very clear that time-limited moisture-conditioning standards such as ISO-62 and ASTM D570-98 are not appropriate for measuring moisture absorption or mechanical properties on nanocomposites. This type of methods might give the impression that nanocomposites absorb less water, while the presented results show that only the speed of water absorption is different.

4.1.2. Aspect ratios

The aspect ratios described in this paper are the effective aspect ratio of the particles present in the nanocomposite, not of the primary silicate sheets.

The aspect ratios of the platelets (Fig. 7) are calculated from the diffusion coefficients for the matrix and the nanocomposites, using Eq. (4).

In Fig. 7 two lines are drawn as a best fit through the average aspect ratios of Somasif® MAE, and through the combined results of Cloisite® 30B and Nanomer® I30TC. The calculated aspect ratios suggest that Somasif® MAE particles have a lower average aspect ratio than the other two ($\sim$1/2), which can be caused by a reduced degree of exfoliation in the MAE nanocomposites. Visual indications for the imperfect exfoliation were seen in the melt: the MAE nanocomposite showed

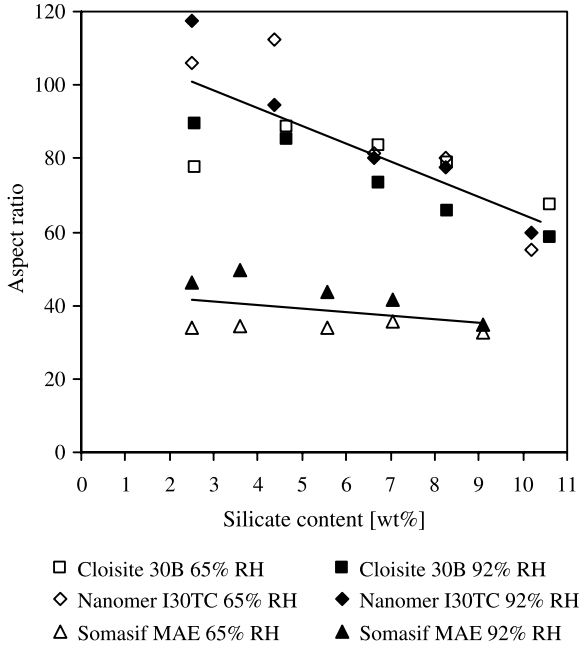

Fig. 7. Aspect ratios calculated from diffusion coefficients.

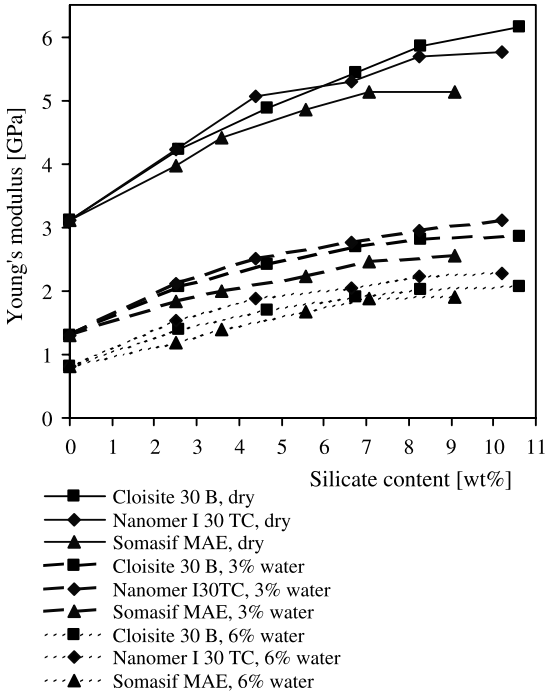

Fig. 8. Young's modulus versus silicate content for various moisture contents.

a much lower melt viscosity and an opaque instead of a transparent melt. The fact that Somasif® MAE has two aliphatic chains on each quaternary ammonium group in instead of one for the Cloisite® 30B and Nanomer® I30TC samples, is probably the cause of the reduced exfoliation. The double amount of chains leaves less space for interactions of polymer chains with the silicate surface and provides a more hydrophobic surface than surfactants with a single chain. In general, relatively hydrophilic modified layered silicates have a better interaction with the hydrophilic PA6 chains [30].

Another general trend that can be seen in Fig. 7 is the decrease of the calculated aspect ratios with increasing silicate content. This could be caused by reduced exfoliation and can be an explanation for the observation that the effectiveness of reinforcement in nanocomposites is often reduced at high silicate content [7,15,16,31].

4.2. Mechanical properties

4.2.1. Modulus

The tensile moduli of the nanocomposites at various moisture contents are shown in Fig. 8.

It is found that the two different montmorillonite-based fillers (Cloisite® 30B and Nanomer® I30TC) give more or less equal moduli, while Somasif® MAE synthetic mica gives a slightly lower modulus. This is in agreement with the results for the diffusion coefficients and aspect ratios, and is probably the result of imperfect exfoliation of the MAE nanoparticles.

When the samples are moisture conditioned, the modulus of PA6 and the nanocomposites is significantly reduced. The reduction of the modulus in the presence of water is common to all polyamides to a certain degree, and it is caused by the plasticizing action of water molecules in polyamides [32]. All polyamides form hydrogen bonds between the amide groups, and water can bind in between these hydrogen-bonding groups [1]. This increases the mobility of the polymer chains due to weaker interactions, causing a reduction of the glass transition temperature. PA6 has a glass transition temperature around 60 °C in dry conditions, but in moisture conditioned samples this can decrease to room temperature and below [1]. The associated drop of the modulus around T_g can be seen in Fig. 9.

The presence of the silicate filler does not change T_g and the amount of T_g reduction due to moisture conditioning is similar for nanocomposites and unfilled PA6 (Fig. 9). Both samples show that the reduction of the modulus at room temperature is due to the reduction of T_g. Far above T_g the modulus is not affected much and far below T_g the modulus shows a slight increase, which has been reported before [1]. The importance of the modulus enhancement for the temperature range at which PA6 nanocomposites will often be used can be seen in Fig. 9. If for a certain application a modulus value of for example at least 1 GPa is necessary, Fig. 9 shows that nanocomposites can provide a very large increase in the temperature range at which a material can be applied, up to 100 °C higher. This is closely related to the observed increase in the heat distortion temperature (HDT). The behaviour of T_g in PA6 explains the amount of modulus reduction found for various moisture contents as shown in Fig. 8. The modulus reduction upon addition of the first 3% water has a larger influence on the modulus than the addition of large amounts of water, because the addition of the first 3% water causes the T_g to decrease to around the testing temperature.

The reduced water absorption speed, combined with the influence of moisture on the T_g and modulus has important implications for the use of PA6 nanocomposites. This is illustrated by the moduli of samples that have been exposed for

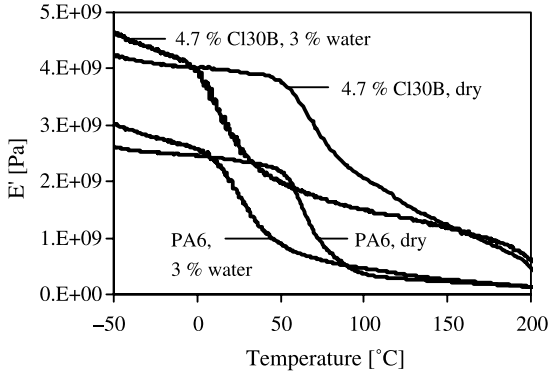

Fig. 9. Storage modulus from DMA for dry and moisture conditioned PA6 and 4.7 wt% Cloisite 30B nanocomposite.

270 days to standard atmospheric conditions (ca. 20 °C—50% RH), shown in Fig. 6. The moduli of the nanocomposites is hardly reduced after this long time, unlike the unfilled PA6. However, with the diffusion coefficients of the nanocomposites (Fig. 4) and the influence of temperature (Fig. 5) it can be estimated that it will take a few years to reach moisture saturation, and thus the modulus of the nanocomposites will eventually drop.

4.3. Yield and fracture behaviour

In Fig. 10 the yield or fracture stress of all the samples is shown. The solid points show yield stresses (the maximum in the stress–strain curve), the open points show the brittle fracture stress if the yield point was not reached.

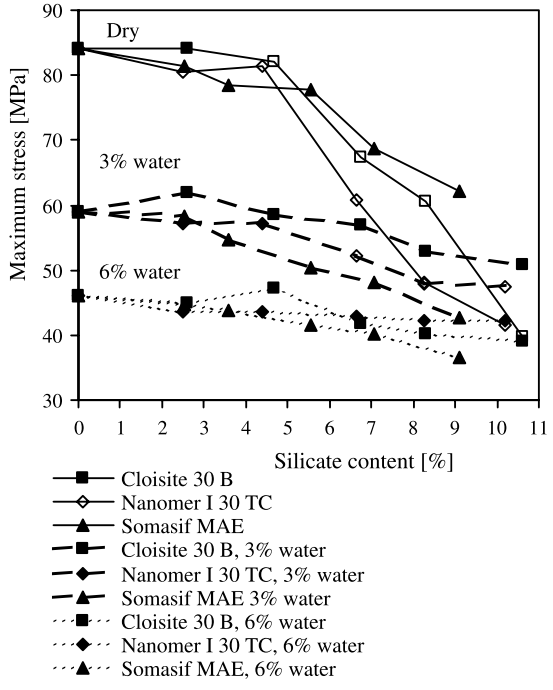

Fig. 10. Maximum stress versus silicate concentration for various moisture contents. Closed symbols represent the yield stress, open symbols the brittle fracture stress when the yield point was not reached.

In general, increasing the silicate content causes more brittle fracture behaviour, while increasing the moisture content causes a reduction of the yield stress and more ductile fracture behaviour. The ductile behaviour of wet samples could have been expected because this lowers the T_g, which increases the chain mobility of the amorphous phase. There seems to be a trade-off between modulus and ductility; the samples with the highest modulus show the most brittle fracture behaviour. The nanocomposites based on Nanomer® I30TC are most brittle, they are all brittle in the dry state and the samples with 3% water are brittle above 4.4% silicate. The less perfectly exfoliated Somasif® MAE nanocomposites show ductile fracture behaviour up to 9% silicate, even in the dry state. This ductile yield behaviour is accompanied by a reduction of the yield stress with increasing silicate content. A decrease in yield stress can be an indication of a weak adhesion between the particles and the matrix polymer. Rigid particles with a weak interaction with the polymer can de-bond from the matrix at a stress below the yield point. This results in small voids in the polymer and this can reduce the yield stress and increase the ductility, in the same way as cavitated rubber particles in impact modified blends [33–35]. The de-bonding mechanism seems to play a role in the Somasif® MAE nanocomposites, illustrated by the stress whitening that was visible just before the yield stress was reached. Well-bonded particles do not de-bond from the matrix at stress levels below the yield stress and are, therefore, not capable of decreasing the yield stress of the samples. The less exfoliated particles like Somasif® MAE in PA6 give a smaller increase in modulus, but they do not cause brittle fracture behaviour, which can be an important advantage. However, the nanocomposite samples that were kept for 270 days at atmospheric conditions were all brittle (results not shown), including the MAE nanocomposites, despite the absorption of a small amount of water. This change in ductility could be a result of the physical aging of the polymer during this period. The increase in the density of the amorphous phase due to molecular re-arrangements associated with physical aging [32,36], can cause a reduction of the ductility. This can counteract the increased mobility and ductility caused by the absorption of water.

5. Conclusions

The nanocomposites absorb water at a slower rate than the unfilled PA6 samples, as expected. However, when given sufficient time the nanocomposites are capable of absorbing similar quantities of water in the matrix phase as the unfilled polymer. The diffusion coefficients of the nanocomposites are reduced to approximately 1/3 of the original value at the highest silicate loading. The conditioning temperature has a much stronger influence on the time needed to reach saturation. Therefore, increased temperature conditioning is necessary with samples of several mm thick; in moderate conditions (20 °C—50% RH) the samples absorb moisture so slowly that it takes very long times, up to several years for

nanocomposites, to reach complete saturation. Constant monitoring of the weight-increase should be used to determine if the equilibrium has been reached. The moisture absorption results show that time-limited moisture absorption standards like ISO-62 and ASTM D570-98 are not suitable to compare unfilled polymers with nanocomposites, because they would give a wrong impression of the moisture absorption capabilities

The modulus of the nanocomposites increases continuously with increasing silicate content, at around 10 wt % the moduli of the Cloisite® and Nanomer® nanocomposites are twice that of the unfilled resin. At higher silicate content the modulus increase levels off, while the Somasif® MAE nanocomposites have a lower modulus at all concentrations, probably due to reduced exfoliation.

The modulus of moisture-conditioned nanocomposites shows a reduction just like the unfilled polymer. At around 6% silicate the modulus of the moisture conditioned nanocomposite is equal to the modulus of the dry unfilled polymer (at room temperature). This way one of the main drawbacks of polyamides, the large decrease of the modulus in wet conditions, can be compensated by the addition of a small quantity of exfoliated silicate.

The fracture behaviour of the nanocomposites is influenced by the type and concentration of filler, the moisture content and the aging time. In general the addition of silicate filler reduces the ductility, in the dried samples only the Somasif® MAE samples and the lowest concentration of Cloisite® 30B were ductile. Nanomer® I30TC gave the most brittle samples; even at a moisture content of 3% they were all brittle while all the other samples were completely ductile at that water content. At a moisture level of 6% all samples were ductile. The fact that the Somasif® MAE nanocomposites tested after conditioning for 270 days at atmospheric conditions were brittle while the fresh dry samples were ductile shows that physical aging also has an influence on ductility. The physical aging properties of nanocomposites have been investigated in more detail using creep measurements and the results will be published soon in this journal.

From the ratio of the matrix and composite diffusion coefficients the average aspect ratio can be estimated. The aspect ratios from the diffusion coefficients are around 100 in the low concentration and decrease somewhat at higher filler levels to around 70. The MAE nanocomposites show lower aspect ratios, which can be explained by the reduced interaction with the polymer.

Remarkably, the aspect ratios as calculated from diffusion data shows a good agreement with aspect ratios calculated from mechanical properties using the Halpin–Tsai composite model and from melt rheology measurements [15,37].

The combined results of moisture diffusion in PA6 nanocomposites and the influence of moisture on the mechanical properties as presented in this paper, indicate that parts with a thickness of several millimetre will be subject to large changes in (mechanical) properties over long time periods. Polyamide parts and especially nanocomposites will be in a non-equilibrium state during moisture absorption, leading to constantly changing mechanical properties for periods up to several years. The modulus will eventually drop after enough moisture is absorbed to lower T_g below the use temperature, and the fracture behaviour will probably become more ductile at that point. It has to be realized that besides the moisture absorption, also physical aging plays an important role in the development of the properties of PA 6 nanocomposites over long time scales. However, the reduced moisture transport rate of nanocomposites means that the properties will be less sensitive to short term fluctuations in environmental conditions than unfilled polyamide. Pre-conditioning at elevated temperatures can speed up the moisture absorption process and lead to more stable and predictable properties.

Acknowledgements

The work of D.P.N. Vlasveld, J. Groenewold and S.J. Picken forms part of the research program of the Dutch Polymer Institute (DPI), project number 279. The authors would like to thank Reinoud Gaymans and the University of Twente for the use of their injection moulding equipment.

References

[1] Kohan MI. Nylon plastics handbook. Munich: Carl Hanser; 1995.
[2] Kojima Y, Usuki A, Kawasumi M, Okada A, Fukushima Y, Kurauchi T, et al. J Mater Res 1993;8(5):1185–9.
[3] Usuki A, Kawasumi M, Kojima Y, Okada A, Kurauchi T, Kamigaito O. J Mater Res 1993;8(5):1174–8.
[4] Usuki A, Kojima Y, Kawasumi M, Okada A, Fukushima Y, Kurauchi T, et al. J Mater Res 1993;8(5):1179–84.
[5] Vaia RA, Giannelis EP. Macromolecules 1997;30(25):8000–9.
[6] Kawasumi M, Hasegawa N, Kato M, Usuki A, Okada A. Macromolecules 1997;30(20):6333–8.
[7] Akkapeddi MK. Polym Compos 2000;21(4):576–85.
[8] Cho JW, Paul DR. Polymer 2001;42(3):1083–94.
[9] Giannelis EP. Adv Mater 1996;8(1):29.
[10] Es MAv, Xiqiao F, Turnhout Jv, Giessen Evd. Comparing polymer-clay nanocomposites with conventional composites using composite modeling. Specialty polymer additives. Oxford: Blackwell Science; 2001.
[11] Kojima Y, Usuki A, Kawasumi M, Okada A, Kurauchi T, Kamigaito O. J Appl Polym Sci 1993;49(7):1259–64.
[12] Murase S, Inoue A, Miyashita Y, Kimura N, Nishio Y. J Polym Sci, Part B: Polym Phys 2002;40(6):479–87.
[13] Liu XH, Wu QJ. Macromol Mater Eng 2002;287(3):180–6.
[14] Wang H, Zeng CC, Elkovitch M, Lee LJ, Koelling KW. Polym Eng Sci 2001;41(11):2036–46.
[15] Vlasveld DPN, Groenewold J, Bersee HEN, Mendes E, Picken SJ. Polymer 2005;46(16):6102–13.
[16] Es MAv. Polymer clay nanocomposites. The importance of particle dimensions. Thesis. Delft University of Technology; 2001.
[17] Akzo Nobel Surface Chemistry website; 2004.
[18] Fornes TD, Paul DR. Polymer 2003;44(14):3945–61.
[19] Rothon R. Particulate-filled polymer composites. New York: Longman; 1995.
[20] Crank J. The mathematics of diffusion. Oxford: Oxford University Press; 1975.
[21] Nielsen LE. J Macromol Sci, Part A 1967;5(1):929–42.

[22] Lincoln DM, Vaia RA, Wang ZG, Hsiao BS, Krishnamoorti R. Polymer 2001;42(25):9975–85.
[23] Brydges WT, Gulati ST, Baum G. J Mater Sci 1975;10(12):2044–9.
[24] Hatta H, Taya M, Kulacki FA, Harder JF. J Compos Mater 1992;26(5): 612–25.
[25] Kojima Y, Usuki A, Kawasumi M, Okada A, Kurauchi T, Kamigaito O, et al. J Polym Sci, Part B: Polym Phys 1995;33(7):1039–45.
[26] Varlot K, Reynaud E, Kloppfer MH, Vigier G, Varlet J. J Polym Sci, Part B: Polym Phys 2001;39(12):1360–70.
[27] Fornes TD, Paul DR. Polymer 2003;44(17):4993–5013.
[28] Hanspach J, Pinno F. Acta Polym 1992;43(4):210–3.
[29] Lim LT, Britt IJ, Tung MA. J Appl Polym Sci 1999;71(2):197–206.
[30] Fornes TD, Hunter D, Paul DR. Macromolecules 2004;37(5):1793–8.
[31] Liu L, Qi Z, Zhu X. J Appl Polym Sci 1999;71:1133–8.
[32] Struik LCE. Polymer 1987;28(9):1521–33.
[33] Zuiderduin WCJ, Westzaan C, Huetink J, Gaymans RJ. Polymer 2003; 44(1):261–75.
[34] Wilbrink MWL, Argon AS, Cohen RE, Weinberg M. Polymer 2001; 42(26):10155–80.
[35] Zuiderduin WCJ, Vlasveld DPN, Huetink J, Gaymans RJ. Polymer 2004; 45(11):3765–79.
[36] Spinu I, McKenna GB. Polym Eng Sci 1994;34(24):1808–14.
[37] Vlasveld DPN, Jong Md, Bersee HEN, Gotsis AD, Picken SJ. Polymer 2005;46(23):10279–89.